

**Sensitivity analysis  
for BERLIOZ**

K. Nester and  
H.-J. Panitz

# Sensitivity analysis by the adjoint chemistry transport model DRAIS for an episode in the Berlin ozone (BERLIOZ) experiment

**K. Nester and H.-J. Panitz**

Institut für Meteorologie und Klimaforschung (IMK), Forschungszentrum Karlsruhe/Universität  
Karlsruhe, Hermann-von-Helmholtz-Platz 1, 76344 Eggenstein-Leopoldshafen, Germany

Received: 2 May 2005 – Accepted: 1 July 2005 – Published: 13 September 2005

Correspondence to: K. Nester (klaus.nester@imk.fzk.de)

© 2005 Author(s). This work is licensed under a Creative Commons License.

Title Page

Abstract

Introduction

Conclusions

References

Tables

Figures

◀

▶

◀

▶

Back

Close

Full Screen / Esc

Print Version

Interactive Discussion

EGU

## Abstract

The Berlin Ozone Experiment (BERLIOZ) was carried out in summer 1998. One of its purposes was the evaluation of Chemistry Transport Models (CTM). CTM KAMM/DRAIS was one of the models considered. The data of 20 July were selected for evaluation. On that day, a pronounced ozone plume developed downwind of the city. Evaluation showed that the KAMM/DRAIS model is able to reproduce the meteorological and ozone data observed, except at distances far downwind of the city (60–80 km). In that region, the DRAIS model underestimates the measured ozone concentrations by approx. (10–15) ppb.

Therefore, this study was conducted to detect possible reasons for this deviation. A comprehensive sensitivity analysis was carried out, to determine the most relevant model parameters. The adjoint DRAIS model was developed for this purpose, because the most effective method of calculating the sensitivities is the application of the adjoint model. The least squares of the measured and simulated ozone concentrations between 08.0 UTC and 16.0 UTC at two stations 30 km and 70 km downwind of the city centre were chosen as the distance function. The model parameters considered in this study are the complete set of initial and boundary species concentrations, emissions, and reaction rates, respectively. A sensitivity ranking showing the relevance of the individual parameters in the set is determined for each parameter set.

In order to find out which modification in the parameter sets most reduces the distance function, simplified 4-D data assimilation was carried out. The result of this data assimilation shows that modifications of the reaction rates provide the best agreement between the measured and the simulated ozone concentrations at both stations. However, agreement is still acceptable when the parameters in the other sets are modified together. The investigation demonstrates that an analysis of this type can help to explain inconsistencies between observations and simulations. The analysis also shows, however, that the parameters responsible cannot be determined unequivocally.

### Sensitivity analysis for BERLIOZ

K. Nester and  
H.-J. Panitz

Title Page

Abstract

Introduction

Conclusions

References

Tables

Figures

◀

▶

◀

▶

Back

Close

Full Screen / Esc

Print Version

Interactive Discussion

## 1. Introduction

The Berlin Ozone (BERLIOZ) Experiment (Becker et al., 1999) was carried as part of the German Tropospheric Research Programme (TSF) in the period between 13 July and 9 August 1998. The experimental domain comprised the city of Berlin and an area within a radius of approx. 100 km around the city. The experiment mainly served to study the transport and chemical transformation processes in the urban plume of Berlin under photo-smog conditions. The study focused on the production of ozone and other oxidants. However, the data also were to be used for evaluating Chemical Transport Models (CTM). As the chemical production of oxidants, especially ozone, depends on a large number of parameters, many experiments have been carried out to analyze the relevance of the processes involved. Urban plumes are of special interest because of their limited extension and the possibility to relate the plume to the emissions from the city. Unlike other experimental sites in Europe located in complex terrain, e.g. Athens (Peleg et al., 1997), Madrid (Plaza et al., 1997), Milan (Prevot et al., 1997) and Vienna (Wotava et al., 1998), Berlin was selected because of its location in a flat environment extending approximately 100 km around the city. The urban plume is not influenced by any other major sources in many directions.

In an earlier study, a simulation by the KAMM/DRAIS model was conducted for 20 July (Nester et al., 2000). Its results were compared with measured meteorological and chemical data. As in the investigation by Memmesheimer et al. (1997), additional mass budget simulations were performed (Panitz and Nester, 2002) to determine the relevant processes as function of time and space. Those evaluations showed the KAMM/DRAIS model to be able to reproduce the data observed, except for the ozone concentrations at greater distances 60–80 km downwind of the city of Berlin. In this region, the model underestimated the observed ozone concentrations by 10–15 ppb. Statistical investigation of the uncertainties inherent in the DRAIS model (Nester and Panitz, 2004) with respect to ozone shows that such deviations occur during daytime in some 25% of the cases compared. Although this is not a rare incidence, there seems

### Sensitivity analysis for BERLIOZ

K. Nester and  
H.-J. Panitz

Title Page

Abstract

Introduction

Conclusions

References

Tables

Figures

◀

▶

◀

▶

Back

Close

Full Screen / Esc

Print Version

Interactive Discussion

to be a defect in the model proper or in the model parameters, because this deviation is restricted to one particular region.

The main purpose of this investigation is identifying possible reasons for the deviations between the observed and the calculated ozone concentrations in the city plume at greater distances. Also, it is of general interest to quantify those model parameters which could most likely be responsible for the deviations. In order to determine the most relevant parameters, a sensitivity analysis was carried out. The model parameters considered at each grid point of the model domain are the initial and the boundary conditions of the species concentrations, emissions, and reaction rates. The most effective method of determining sensitivities is by applying the adjoint DRAIS model developed for this specific purpose. Besides determining sensitivities, a simplified data assimilation was carried out to identify those parameter uncertainties which probably cause the discrepancies between the measured and the simulated ozone concentrations.

## 2. Simulations by the KAMM/DRAIS model and results

### 2.1. The KAMM/DRAIS model system

The KAMM/DRAIS model system (Fig. 1) consists of the KAMM meteorological model (Adrian and Fiedler, 1991) and the DRAIS dispersion model (Nester and Fiedler, 1992). The KAMM non-hydrostatic Eulerian model solves the Navier-Stokes equations of motion, the continuity equation, and the heat equation in a terrain following coordinate system, which allows better resolution close to the ground than at higher levels. A soil-vegetation model (Schädler et al., 1990) describes the interaction between the soil and the atmosphere.

The DRAIS dispersion model solves the diffusion equation on an Eulerian grid by using the same terrain following coordinate system as the KAMM model. Dry depositions of the different species are modelled by their dry deposition velocities (Baer and

## Sensitivity analysis for BERLIOZ

K. Nester and  
H.-J. Panitz

Title Page

Abstract

Introduction

Conclusions

References

Tables

Figures

◀

▶

◀

▶

Back

Close

Full Screen / Esc

Print Version

Interactive Discussion

Nester, 1992). The gas phase chemical reaction mechanism of the RADM2 model (Stockwell et al., 1990) is applied to simulate chemical processes.

A local first order approach is chosen for vertical diffusion in the stable and neutral boundary layer. A non-local similarity approach is used in the convective boundary layer (Degrazia, 1988).

A special module can be employed to calculate the components of the mass budget in predefined volumes for all species considered in the model (Panitz et al., 1997).

## 2.2. Simulations

Simulations by the KAMM/DRAIS model system were carried out for 20 July 1998. The model domain had a size of 200 km×200 km. The city of Berlin was located in the centre of the domain. Horizontal grid resolution was 2 km. The external forcing for the KAMM model and the initial conditions and the boundary conditions for the species concentrations in the DRAIS model were determined from the results of the European scale EURAD model (Ebel et al., 1997). The grid size for this simulation was 18 km. Only the ozone profile at the upper levels (1.5–5 km) was modified in line with the measurements run by the IBUG aircraft (Corsmeier et al., 2002). The emission data for this episode were provided by IER, Stuttgart. Land use and topography data were taken from the database supplied by IMK–IFU, Garmisch-Partenkirchen.

The ozone concentration distribution near ground level at 15.0 UTC on 20 July 1998, shows a pronounced ozone plume downwind of the city of Berlin (Fig. 2). The maximum ozone concentration in this plume is 68 ppb. It occurs at a distance of about 70 km. Air masses with high ozone concentrations are transported over the southern boundary of the model domain.

The diurnal ozone concentration cycles at two stations are presented in Fig. 3. At the Eichstaedt station, roughly 30 km downwind of the city centre of Berlin, the simulated ozone concentrations fit measurements quite well. At Menz station, however, about 70 km downwind of the city centre, the simulated ozone concentrations underestimate the measured ones. A similar result is obtained when comparing the ozone

### Sensitivity analysis for BERLIOZ

K. Nester and  
H.-J. Panitz

Title Page

Abstract

Introduction

Conclusions

References

Tables

Figures

◀

▶

◀

▶

Back

Close

Full Screen / Esc

Print Version

Interactive Discussion

---

**Sensitivity analysis  
for BERLIOZ**

K. Nester and  
H.-J. Panitz

---

[Title Page](#)[Abstract](#)[Introduction](#)[Conclusions](#)[References](#)[Tables](#)[Figures](#)[◀](#)[▶](#)[◀](#)[▶](#)[Back](#)[Close](#)[Full Screen / Esc](#)[Print Version](#)[Interactive Discussion](#)

EGU

concentrations measured along the flight track of the IBUF aircraft (see Fig. 2) with the corresponding simulated concentrations. The main flight track begins on the upwind side approx. 50 km southwest of Berlin, crosses the city, and ends at about 100 km downwind. Along this flight track, the aircraft flew at different altitudes. As can be seen from Fig. 4, the wind direction measured during the flight is simulated well by the model. A similar agreement is found for the wind speed. The simulated ozone concentration along the flight track also agrees quite well with the observations, except for two time periods (13.8 UTC and 15.1 UTC). During these two periods, the aircraft flew in the area around and north of Menz where the model underestimates the measured ozone values by approx. 10–15 ppb (Fig. 5) while the meteorological conditions are simulated well.

### 2.3. Mass budget components of ozone in four layers over three regions

The mass budget module in the KAMM/DRAIS model calculates the contributions by the different processes to the change in the mean concentration in a predefined volume (Fig. 6). Production and loss terms are marked P and L, respectively. More details are published in Panitz and Nester (2002).

The calculations were performed for three regions in the urban plume. The first region comprises the city of Berlin, two others are located north of the first region (Fig. 7). The atmospheric column over each region was divided into four vertical layers:

Layer 1: 2000 m–5000 m (free troposphere)

Layer 2: 1200 m–2000 m (upper boundary layer)

Layer 3: 75 m–1200 m (lower boundary layer)

Layer 4: ground–75 m (surface layer)

Although all mass budget components were determined, only the changes in ozone concentration due to chemical transformations are presented. Determining this quantity was one of the purposes of the experiment. Figure 8 shows the hourly change in the chemical ozone production rate in layer 3. In regions 1 and 2, nearly the same production rates are calculated, whereas the production rate in region 3 obviously is

lower in the afternoon.

On the downwind side of the city, the ozone production in the urban plume as derived from aircraft measurements (IBUF) in the afternoon reaches a level of approx.  $(6.5 \pm 1.0)$  ppb/h (Corsmeier et al., 2002). The aircraft flew at different levels in layer 3, crossing regions 2 and 3 several times. Averaging the simulated ozone production rate over the corresponding periods results in 5.1 ppb/h and 3.5 ppb/h for regions 2 and 3, respectively. For region 2, this is still in acceptable agreement with the corresponding levels derived from the aircraft measurements. The ozone production rate in region 3 obviously is too low. Comparison for the city results in  $(4.5 \pm 1.0)$  ppb/h and 5.0 ppb/h for the measured and the simulated ozone production rates, respectively.

This result indicates that the ozone concentrations measured at Menz are underestimated because the ozone production rate is too low in the model.

### 3. Sensitivity analysis

A sensitivity study was performed to find the reasons of the discrepancies identified in ozone concentrations. Four parameters were selected for analysis:

- emissions,
- initial species concentrations,
- boundary species concentrations,
- reaction rates.

In our case, sensitivity is defined as the parameter derivative,  $\partial DF / \partial P$ , of a distance function,  $DF$ . The value of the distance function describes the quality of the agreement between the measured and the calculated ozone concentrations at the Eichstaedt and

## Sensitivity analysis for BERLIOZ

K. Nester and  
H.-J. Panitz

Title Page

Abstract

Introduction

Conclusions

References

Tables

Figures

◀

▶

◀

▶

Back

Close

Full Screen / Esc

Print Version

Interactive Discussion

Menz stations in the daytime. It is defined as

$$DF = \sum_{l=1}^2 \sum_{i=8}^{16} (C_{s,i} - C_{m,i})_l^2 \quad (1)$$

with

$C_{s,i}$  : simulated ozone concentration for the time  $i$  (UTC),

$C_{m,i}$  : measured ozone concentration for the time  $i$  (UTC),

$l=1$  : at Eichstaedt station (see Figs. 2 and 3),

$l=2$  : at Menz station (see Figs. 2 and 3).

Both stations were selected in order to allow the ozone concentrations in the plume closer and farther away from the city of Berlin to be considered simultaneously. This is important especially for the simplified data assimilation in Sect. 4.

The most effective way of calculating the sensitivities is based on application of the adjoint model. A fundamental study with emissions as a parameter was published by Elbern et al. (2000). A tracer transport study on a global scale was performed earlier by Pudykiewicz (1998). Studies with distance functions based on ozone concentrations were carried out by Elbern and Schmidt (2001), using the initial species concentrations as a model parameter, and by Schmidt and Martin (2003) with the emissions as a parameter. Other studies of this kind were published by Vautard et al. (2000), based on emissions and reaction rates as the model parameters, and Menut (2003) investigating the sensitivity of a larger number of relevant parameters. Also the adjoint method was applied to optimize the location of observations (Daescu and Carmichael, 2002).

The adjoint DRAIS model therefore was developed for the sensitivity study.

### 3.1. The adjoint DRAIS model

The adjoint model can be derived from the tangent linear model. The variables of the latter model are the gradients of the variables of the original model related to a model

## Sensitivity analysis for BERLIOZ

K. Nester and  
H.-J. Panitz

Title Page

Abstract

Introduction

Conclusions

References

Tables

Figures

◀

▶

◀

▶

Back

Close

Full Screen / Esc

Print Version

Interactive Discussion

parameter. The definitions of adjoint(\*) operators and variables are given by Eq. (2).

$$\langle G^*; LG \rangle = \langle G; L^*G^* \rangle, \quad (2)$$

with

$\langle A; B \rangle$ : inner product of  $A$  and  $B$

$G = \partial C / \partial P$ : derivative of the concentrations,  $C$ , related to a model parameter,  $P$ , which is the variable in the tangent linear DRAIS model.

$G^*$  = adjoint of  $G$ ,

$L$  = operator of the differential equations in the tangent linear DRAIS model

$L^*$  = operator of the differential equations in the adjoint DRAIS model.

Although programmes exist for automatic transformation of the original code into the tangent linear and the adjoint codes (TAMC, Giering and Kaminski, 1998; Odyssee, Rostaing et al., 1993), the adjoint DRAIS model was developed manually. Unlike the adjoint CHIMERE model (Schmidt and Martin, 2003), however, it is not coded line by line in accordance with the principles of automatic transformation. The adjoint DRAIS model is derived from the tangent linear model of DRAIS, which uses the same difference approximations as the original model. The equation defining the adjoint operators and variables (Eq. (2)) is applied to determine the adjoint DRAIS model as in the procedure given by Ustinov (2001). Instead of the differential equations, the difference equations are used to obtain the adjoint difference equations. This is advantageous because the results of the sensitivity analysis can be better compared with the calculated sensitivities using the tangent linear and the original models. The adjoint DRAIS model is coded in a similar way as the original model and the tangent linear model. Of course, the subprograms are arranged in inverse order. These manually coded programmes offer the advantage of clear structures and can be optimized with respect to storage requirements and computing time (Elizondo et al., 2002).

## Sensitivity analysis for BERLIOZ

K. Nester and  
H.-J. Panitz

Title Page

Abstract

Introduction

Conclusions

References

Tables

Figures

◀

▶

◀

▶

Back

Close

Full Screen / Esc

Print Version

Interactive Discussion

## Sensitivity analysis for BERLIOZ

K. Nester and  
H.-J. Panitz

Title Page

Abstract

Introduction

Conclusions

References

Tables

Figures

◀

▶

◀

▶

Back

Close

Full Screen / Esc

Print Version

Interactive Discussion

### 3.1.1. Advection scheme

In the original DRAIS model, a second-order non-oscillatory Flux Corrected Transport (FCT) advection scheme with limiters is implemented. In addition, divergence correction is used. To avoid problems in the adjoint scheme (Thuburn and Haine, 2001), this scheme was used without limiters. It is now linear and of second order, but no longer monotone. The results of the original and the modified advection schemes differ only slightly. The distance function (Eq. (1)) decreases by only approx. 3%. The adjoint advection term was derived from Eq. (2) with the modified difference scheme used for advection. It differs slightly from the tangent linear advection scheme with inverse velocities. The divergence correction term is omitted in the adjoint advection scheme.

### 3.1.2. Diffusion scheme

Diffusion is approximated in the original and the tangent linear models by a centred difference scheme. This scheme can be used without any modification also in the adjoint DRAIS model. Only the lower boundary condition differs from that of the tangent linear model. The reason for this modification lies in the formulation of the flux at the lower boundary, which is defined as

$$FLUX_g = V_d * C \quad (3)$$

with

$FLUX_g$  = species concentration flux to the ground,

$C$  = species concentration,

$V_d$  = deposition velocity.

$V_d$  and  $C$  are determined at a reference level above ground and not directly on the ground, which is the lowest level in the DRAIS model. This implies an adjoint boundary condition with a slightly modified deposition velocity.

### 3.1.3. Chemical reaction terms

The chemical reaction terms in the original DRAIS model are non linear. They are linearized in the tangent linear model. The linearized chemical reaction terms can be written as an  $n * n$  matrix (Eq. (4)), where  $n$  is the number of variables,  $\partial C_k / \partial P$ , in the tangent linear model.

$$d(\partial C_k / \partial P) / dt = \sum_{i=1}^n A_{k,i} \partial C_{k,i} / \partial P \quad k = 1, n. \quad (4)$$

These variables are the model parameter derivatives of the chemical species concentrations in the original DRAIS model. 41 transported and 18 diagnosed species are considered in the DRAIS model. This means that  $n$  is 59. In the adjoint DRAIS model, the transpose of this matrix is employed. The solving procedure is the same in both models and corresponds to the QSSA method of the RADM2 module (Chang et al., 1987) used in the original DRAIS model.

### 3.1.4. Test calculations

The adjoint DRAIS model was tested by sensitivity calculations for a large number of model parameters at different grid points. The sensitivities of the distance function calculated by applying the adjoint DRAIS model are compared with the sensitivities derived from two simulations with the original model using the parameter values,  $P \pm \Delta P$ . Of course, the results cannot be identical, but tests have shown that the relative error should be less than 1%, at least for the higher sensitivity values. It is important to check the sensitivity for different parameters at various grid points, because good agreement may be obtained for some sensitivities although there is still an error in the code. The results of the adjoint model were also checked by those of the tangent linear model.

## Sensitivity analysis for BERLIOZ

K. Nester and  
H.-J. Panitz

Title Page

Abstract

Introduction

Conclusions

References

Tables

Figures

◀

▶

◀

▶

Back

Close

Full Screen / Esc

Print Version

Interactive Discussion

### 3.2. Results of sensitivity analysis

The sensitivity of the distance function relative to the parameters mentioned above is calculated for each grid point. For these calculations, the grid size was increased by a factor of 10 because of the large number of data to be stored. In addition, the simplified data assimilation (Sect. 4) takes a lot of computing time. The increase in grid size allows a larger number of simulations with reduced storage and CPU time requirements. Also, more test calculations can be performed. The KAMM/DRAIS simulations (Sect. 2.2) were repeated with a coarse horizontal resolution of 20 km. During the day both stations show only minor differences between the diurnal cycles of ozone concentration resulting from simulations with grid resolutions of 2 km and 20 km (Fig. 3). Therefore, it may be sufficient to calculate sensitivities with the coarser grid.

The sensitivity,  $S_p$ , of the distance function relative to a model parameter is defined as

$$S_p = \Delta DF / \Delta P, \quad (5)$$

where  $\Delta DF$  = variation of the distance function,  $\Delta P$  = variation of the parameter,  $P$ .

In the analysis below, the parameter,  $P$ , is replaced by the reference value,  $P_o$ , multiplied by a factor, ( $FacP$ ), which is the new parameter replacing  $P$ .

$$P = P_o * FacP$$

$$\Delta P = P_o * \Delta FacP.$$

The sensitivity, Eq. (3), is now defined as

$$S_p = \Delta DF / (\Delta FacP * P_o) = S_{pf} / P_o$$

with

$$S_{pf} = \Delta DF / \Delta FacP. \quad (6)$$

The sensitivity,  $S_{pf}$ , used below, is now related to the parameter,  $FacP$ .

## Sensitivity analysis for BERLIOZ

K. Nester and  
H.-J. Panitz

Title Page

Abstract

Introduction

Conclusions

References

Tables

Figures

◀

▶

◀

▶

Back

Close

Full Screen / Esc

Print Version

Interactive Discussion

### 3.2.1. Emissions

The sensitivity related to emissions,

$$S_{ef} = \Delta DF / \Delta F_{acE} \quad (7)$$

is calculated for all grid points where emissions occur, and for all species emitted. The maximum  $S_{ef}$  for each species is plotted in Fig. 9 arranged by species numbers as in the original DRAIS model listed in Appendix A. As the distance function,  $DF$ , depends on the ozone concentrations, it is no surprise that NO is the most sensitive species. The next positions in sensitivity ranking are occupied by the hydrocarbons, OLT, XYL, OL2, HC5, HC3, HC8, OLI, HCHO, and TOL (see Appendix A for the explanation). CO is still found between HC8 and OLI. Compared to TOL, the sensitivities of the other species emitted are a factor of 2 lower. Negative sensitivity means that an increase in emissions of this species reduces the distance function, thus furnishing better agreement of the measured and the simulated ozone concentrations at the stations Eichstaedt and Menz. To obtain a lower distance function, NO emissions must be reduced while hydrocarbon and CO emissions must be increased.

### 3.2.2. Initial species concentrations

The sensitivity of the initial species concentrations is defined as in the previous case:

$$S_{if} = \Delta DF / \Delta F_{acI} \quad (8)$$

The sensitivities are calculated for all species at each grid point. The maximum sensitivity for each species is selected from these data and plotted in Fig. 10. As the distance function depends on the ozone concentration, ozone is expected to be the most sensitive species. In sensitivity ranking, ozone is followed by PAN, NO<sub>2</sub>, HCHO, OLT CO, NO, and ALD (see Appendix A for the explanation). When individual species are considered, PAN can be seen to play a greater role in ozone chemistry than other species.

## Sensitivity analysis for BERLIOZ

K. Nester and  
H.-J. Panitz

Title Page

Abstract

Introduction

Conclusions

References

Tables

Figures

◀

▶

◀

▶

Back

Close

Full Screen / Esc

Print Version

Interactive Discussion

### 3.2.3. Boundary species concentrations

The sensitivity of the boundary species concentrations is defined in the same way as the previous parameters.

$$Sbf = \Delta DF / \Delta FacB \quad (9)$$

5 Figure 11 shows the maximum sensitivity for all species concentrations transported in the model (Appendix A, Species 1–41). The most sensitive species again is ozone, followed by PAN and NO<sub>2</sub>. This is the same ranking as for the initial conditions, but the sign for the NO<sub>2</sub> sensitivity is different. The next positions in the ranking of boundary species concentrations are held by CO, OLT, HCHO, ALD, and NO. These species can  
10 also be found in the ranking list for the initial conditions, albeit in a slightly different order. The other sensitivities are remarkably lower.

### 3.2.4. Photolysis rates

The sensitivities of the photolysis rates,

$$Spf = \Delta DF / \Delta FacP \quad (10)$$

15 are calculated at all grid points and for all 21 photolysis reactions (Stockwell, 1990). The maximum value for each reaction is plotted in Fig. 12. Sensitivity is dominated by reactions 1 and 11. The corresponding reaction equations are listed in Table 1. The highest sensitivity with a positive sign is number 10, the photolysis of HCHO to H<sub>2</sub> and CO. However, this sensitivity is much lower than those for the previous photolysis rates.

### 20 3.2.5. Reaction rates

140 non photolytic reactions are considered in the RADM2 model. For all these reactions the sensitivities

$$Srf = \Delta DF / \Delta FacR \quad (11)$$

---

## Sensitivity analysis for BERLIOZ

K. Nester and  
H.-J. Panitz

---

Title Page

Abstract

Introduction

Conclusions

References

Tables

Figures

◀

▶

◀

▶

Back

Close

Full Screen / Esc

Print Version

Interactive Discussion

---

**Sensitivity analysis  
for BERLIOZ**K. Nester and  
H.-J. Panitz

---

[Title Page](#)[Abstract](#)[Introduction](#)[Conclusions](#)[References](#)[Tables](#)[Figures](#)[⏪](#)[⏩](#)[◀](#)[▶](#)[Back](#)[Close](#)[Full Screen / Esc](#)[Print Version](#)[Interactive Discussion](#)

EGU

are calculated at each grid point. The maximum sensitivities of the reaction rates for all reactions are plotted in Fig. 13. The eight dominating reactions are listed in Table 1 (the first eight reactions). As expected, the rate of the reaction between  $O_3$  and NO shows the highest sensitivity. As can be seen from Table 1, the higher sensitivities are related to reactions with NO,  $NO_2$ , OH, and  $HO_2$ . These reactions play an important role in ozone chemistry. Most of these reactions are also considered in the sensitivity study by Menut (2003).

#### 4. Variation of relevant parameters

After calculation of the sensitivities it was possible to select the most relevant parameters. They are summarized in Table 1. These parameters are modified at each grid point in an iteration process minimizing the distance function. This procedure is similar to real data assimilation. However, a simplified procedure is applied in this case in which correlations between variations at neighbouring grid points are neglected. The simplified parameter variation provides a lower limit of the distance function. This study was conducted to find out which parameter modifications are able to diminish discrepancies observed in ozone concentrations in the city plume at distances far from Berlin. There is no intention to carry out a full data assimilation for which much more data would have to be included and error correlations would have to be considered. In order to avoid completely unrealistic results parameter variation is limited. The limits for the different parameters are also listed in Table 1.

The limits for emissions are estimated from evaluations of the Augsburg project (Slemr et al., 2002). For  $SO_2$ , NO and  $NO_2$  emissions, the same uncertainty factor of 1.5 is used. This means that the lower limit is  $1/1.5=0.66$  and the upper limit is 1.5. Hydrocarbon and CO emissions are more uncertain. Therefore, a value of 2.0 is chosen, which corresponds to a lower limit of 0.5.

The limits for the initial concentrations are estimated in a similar way. For the initial NO concentration, the same limits are used as for the NO emissions, because the NO

---

**Sensitivity analysis  
for BERLIOZ**K. Nester and  
H.-J. Panitz

---

[Title Page](#)[Abstract](#)[Introduction](#)[Conclusions](#)[References](#)[Tables](#)[Figures](#)[⏪](#)[⏩](#)[◀](#)[▶](#)[Back](#)[Close](#)[Full Screen / Esc](#)[Print Version](#)[Interactive Discussion](#)

EGU

concentrations mainly depend on local emissions. Nester and Panitz (2004), showed that differences of 20% can occur between the measured and the simulated ozone concentrations. Therefore, an uncertainty factor of 1.2 is taken for ozone. The uncertainty in the initial NO<sub>2</sub> concentration lies between the values for NO and those for ozone because it is influenced more by chemical processes and long range transport than is NO. The uncertainty factor for the initial hydrocarbon concentrations should be lower than that of the emissions. Therefore, a value of 1.5 is chosen. This value is taken also for the initial concentrations of PAN and CO.

As it is very difficult to define individual limits for the different parameters, the same limitations were chosen for the boundary conditions and the reaction rates. For both parameter sets, a variation of ±40% is allowed (Menut, 2003). In order to avoid unrealistic parameter modifications, this rough estimate of the limits seems to be acceptable.

For the simulations with the simplified data assimilation the model run starts at 00.0 UTC and ends at 05.0 UTC without any modification. The results of this pre-run are used as initial conditions for a subsequent model run from 05.0 UTC till 21.0 UTC. During this model run the modified parameters are taken into account. The assimilation window lies between 08.0 UTC and 16.0 UTC. Only in this time period, improved agreement between the measured and the simulated ozone concentrations at the stations of Eichstaedt and Menz is assured. It would be interesting to see whether there is better agreement also between 05.0 UTC and 08.0 UTC as well as after 16.0 UTC.

Simplified data assimilation is carried out separately with the initial conditions together with the emissions, as recommended by Elbern and Schmidt (2002), the boundary conditions and the reaction rates, respectively. Iterative reduction of the distance function is performed by the conjugate gradient method using limits. The convergence of the distance function is plotted in Fig. 14.

The boundary conditions furnish the highest minimum of the distance function. This result is not surprising, because it takes longer for modifications in the boundary conditions to cause modifications in ozone concentrations at the two stations considered in the distance function. Moreover, the modifications in ozone concentrations are similar

at both stations. At Menz agreement cannot be improved greatly without overestimating the ozone concentrations at Eichstaedt. These effects are reflected in the modified diurnal cycles of the ozone concentration for both stations drawn in the Fig. 15.

The lowest minimum of the distance function is calculated for the reaction rates. Ozone concentrations at the Menz and Eichstaedt stations based on the modified reaction rates agree quite well with the observations in the assimilation window (Fig. 15). This indicates that uncertainties in the reaction rates may be the cause of the discrepancies in ozone concentration. Varying the emissions together with the initial conditions furnishes less satisfactory agreement than modifying the reaction rates does. When the initial conditions and the boundary conditions as well as emissions are modified simultaneously, agreement is satisfactory, but not as good as with modified reaction rates.

In the late afternoon, after 16.0 UTC (the end of assimilation), the ozone concentrations in the KAMM/DRAIS reference simulation and in all runs with modified parameters converge relatively fast. Especially the increased ozone concentration at the station Menz after 16.0 UTC is not simulated properly either by the reference run or by the runs with modified model parameters. This indicates that other reasons could still be responsible for the discrepancies between the measured and the calculated ozone concentrations at Menz station.

## 5. Conclusions

On 20 July 1998, a day in the BERLIOZ experiment, an ozone plume developed downwind of the city of Berlin. Although the meteorological conditions and ozone concentrations on the upwind side of the city are well simulated by the model, the maximum increase in ozone concentration as observed in the plume is underestimated by (10–15) ppb at distances far from the city (60–80 km). In this area, the model also calculates an ozone production rate lower than that derived from aircraft measurements. A sensitivity analysis was carried out to find the reason for this underestimation. It is based

### Sensitivity analysis for BERLIOZ

K. Nester and  
H.-J. Panitz

Title Page

Abstract

Introduction

Conclusions

References

Tables

Figures

◀

▶

◀

▶

Back

Close

Full Screen / Esc

Print Version

Interactive Discussion

**Sensitivity analysis  
for BERLIOZ**K. Nester and  
H.-J. Panitz

Title Page

Abstract

Introduction

Conclusions

References

Tables

Figures

◀

▶

◀

▶

Back

Close

Full Screen / Esc

Print Version

Interactive Discussion

EGU

on a distance function defined as the sum of the least squares between the measured and the simulated ozone concentrations at the stations of Eichstaedt and Menz in the period between 08.0 UTC and 16.0 UTC. The emissions, initial conditions and boundary conditions, and the reaction rates are taken as model parameters. The highest sensitivities are listed in Table 2 arranged by absolute values.

Only five parameters show a sensitivity of more than  $\pm 100 \text{ ppb}^2$ . The others are a factor of two or more lower. It is not surprising that the first five parameters are the most sensitive ones, being directly related to the concentration or the production of ozone. It was to be expected that other parameters, such as the hydrocarbon and CO emissions, also show relevant sensitivities (Table 2). However, their place in the ranking list and the sensitivity values could not be predicted.

In addition, simplified data assimilations were performed. They were not restricted to the five most sensitive parameters, as the ranking changes during the assimilation process, especially when the limits of the most sensitive parameters are reached. Simplified data assimilation shows that modification of the reaction rates can remarkably reduce the distance function. Simultaneous data assimilation with emissions, initial conditions and boundary conditions as the parameter sets also produces acceptable agreement between the measured and the simulated ozone concentrations, although the value of the distance function is still remarkably higher than with the modified reaction rates. After 16.0 UTC (the end of assimilation), a relatively fast convergence of the ozone concentrations simulated with and without parameter modifications is found at both stations. This fast convergence indicates that other effects may still influence the discrepancies detected in ozone concentrations, especially at the station of Menz.

**References**

Adrian, G. and Fiedler, F.: Simulation of unstationary wind and temperature fields over complex terrain and comparison with observations, Contributions to Atmospheric Physics, 64, 27–48, 1991.

**Sensitivity analysis  
for BERLIOZ**K. Nester and  
H.-J. Panitz

Title Page

Abstract

Introduction

Conclusions

References

Tables

Figures

◀

▶

◀

▶

Back

Close

Full Screen / Esc

Print Version

Interactive Discussion

EGU

- Baer, M. and Nester, K.: Parametrization of trace gas dry deposition velocities for a regional mesoscale diffusion model, *Ann. Geophys.*, 10, 912–923, 1992.
- Becker, K. H., Donner, B., and Gäb, S.: BERLIOZ: A field experiment within the German Tropospheric Research Programme, in: *Proc. of EUROTRAC Symposium 98 2*, edited by: Borrell, P. M. and Borrell, P., WIT-Press, Southampton, 669–672, 1999.
- Chang, J. S., Brost, A., Isaksen, I. S. A., Madronich, S., Middleton, P., Stockwell, W. R., and Walceck, C. J.: A three-dimensional Eulerian acid deposition model: Physical concepts and formulation, *J. Geophys. Res.*, 92, 14 618–14 700, 1987.
- Corsmeier, U., Kalthoff, N., Vogel, B., Hammer, M.-U., Fiedler, F., Kottmeier, Ch., Volz-Thomas, A., Konrad, S., Glaser, K., Neininger, B., Lehning, M., Jaeschke, W., Memmesheimer, M., Rappenglück, B., and Jakobi, G.: Ozone and PAN formation inside and outside of the BERLIN plume-Process analysis and numerical process simulation, *J. Atmos. Chem.*, 42, 289–321, 2002.
- Daescu, D. and Carmichael, G. R.: An adjoint sensitivity method for the adaptive location of the observations in air quality modeling, *J. Atmos. Sci.*, 60, 434–450, 2003.
- Degrazia, G. A.: Anwendung von Ähnlichkeitsverfahren auf die turbulente Diffusion in der konvektiven und stabilen Grenzschicht, dissertation, Fakultät für Physik der Universität Karlsruhe, Institut für Meteorologie und Klimaforschung, 1988.
- Ebel, A., Elbern, H., Feldmann, H., Jakobs, H. J., Kessler, C., Memmesheimer, M., Oberreuter, A., and Piekorz, G.: Air pollution studies with the EURAD model system(3): EURAD-European air pollution dispersion model system, *Mitteilungen aus dem Institut für Geophysik und Meteorologie der Universität Köln*, Heft 120, 172, 1997.
- Elbern, H., Schmidt, H., Talagrand, O., and Ebel, A.: 4D-variational data assimilation with an adjoint air quality model for emission analysis, *Environmental Modelling & Software*, 15, 539–548, 2000.
- Elbern, H. and Schmidt, H.: Ozone episode analysis by four-dimensional variational chemistry data assimilation, *J. Geophys. Res.*, 106, No. D4, 3569–3590, 2001.
- Elbern, H. and Schmidt, H.: The development of a 4d variational chemistry data assimilation scheme for initial value and emission rate estimates, in: *Proceedings of the 6th GLOREAM Workshop*, Aveiro, Portugal, 4–6 September, edited by: Borego, C., Bultjes, P., Miranda, A. I., Santos, P., and Carvalho, A. C., 123–132, 2002.

**Sensitivity analysis  
for BERLIOZ**K. Nester and  
H.-J. Panitz

Title Page

Abstract

Introduction

Conclusions

References

Tables

Figures

◀

▶

◀

▶

Back

Close

Full Screen / Esc

Print Version

Interactive Discussion

Elizondo, D., Cappelaere, B., and Faure, Ch.: Automatic versus manual model differentiation to compute sensitivities and solve non-linear inverse problems, *Computers & Geosciences*, 28, 309–326, 2002.

Giering, R. and Kaminski, T.: Recipes for adjoint code construction, *ACM Transactions on Mathematical Software*, 24(4), 437–474, 1998.

Memmesheimer, M., Ebel, A., and Roemer, F.: Budget calculations for ozone and its precursors: Seasonal and episodic features based on model simulations, *J. Atmos. Chem.*, 28, 283–317, 1997.

Menut, L.: Adjoint modelling for atmospheric pollution process sensitivity at regional scale, *J. Geophys. Res.*, 108, No. D17, ESQ 5, 1-17, 2003.

Nester, K. and Fiedler, F.: Modeling of the diurnal variation of air pollutants in a mesoscale area, *Proceedings of the 9th World Clean Air Congress, Montreal, Vol. 5, Paper-No. IU-16C.02, 1992.*

Nester, K., Fiedler, F. Panitz, H.-J., and Zhao, T.: Simulation of an episode of the BERLIOZ experiment and comparison with measured data, in: *Proceedings 4th GLOREAM Workshop, Cottbus, Germany, 20–22 September 2000*, edited by: Schaller, E., Builtjes, P., and Münzenberg, A., 8–16, 2000.

Nester, K. and Panitz, H.-J.: Evaluation of the chemistry transport model system KAMM/DRAIS based in daytime ground level ozone data, *International Journal of Environment and Pollution*, 22, No. 1/2, 87–107, 2004.

Panitz, H.-J., Nester, K., and Fiedler, F.: Determination of mass balances of chemically reactive air pollutants over Baden-Württemberg (F.R.G.) – Study for the regions around the cities of Stuttgart and Freudenstadt, in: *Air Pollution V*, edited by: Power, H., Tirabassi, T., and Brebbia, C. A., Computational Mechanics Publications, Southampton, Boston, 413–422, 1997.

Panitz, H.-J. and Nester, K.: Mass budget simulations of ozone in the city plume of Berlin for an episode of the BERLIOZ experiment, *Companion CD-ROM of: Midgley, P. and Reuther, M. (Eds.), Transport and Chemical Transformation in the Troposphere, Proceedings of the EUROTRAC Symposium 2002, Garmisch-Partenkirchen, Germany, 11–15 March; see also: [http://www-fzk.imk.uni-karlsruhe.de/fi/fzk/imk/seite\\_1513.php](http://www-fzk.imk.uni-karlsruhe.de/fi/fzk/imk/seite_1513.php), 2002.*

Peleg, M., Luria, M., Sharf, G., Vanger, A., Kallos, G., Kotroni, V., Lagouvardos, K., and Varinou, M.: Observational evidence of an ozone episode over the Greater Athens Area, *Atmospheric Environment*, 31, 3969–3983, 1997.

**Sensitivity analysis  
for BERLIOZ**K. Nester and  
H.-J. Panitz

Title Page

Abstract

Introduction

Conclusions

References

Tables

Figures

◀

▶

◀

▶

Back

Close

Full Screen / Esc

Print Version

Interactive Discussion

- Plaza, J., Pujadas, M., and Artinano, B.: Formation and transport of the Madrid ozone plume, *Journal of Air & Waste Management Association*, 47, 766–774, 1997.
- Prevot, A. S. H., Staehlin, L., Kok, G. L., Schillawski, R. D., Neining, B., Staffelbach, T., Nefel, A., Wernli, H., and Dommen, J.: The Milan photooxidant plume, *J. Geophys. Res.*, 102, 23 375–23 388, 1997.
- 5 Pudykiewicz, J. A.: Application of adjoint tracer transport equations for evaluating source parameters, *Atmospheric Environment*, 32, No. 17, 3039–3050, 1998.
- Rostaing, N., Dalmas, S., and Galligo, A.: Automatic differentiation in Odyssee. *Tellus*, 45A, 558–568, 1993.
- 10 Schädler, G., Kalthoff, N., and Fiedler, F.: Validation of a model for heat, mass and momentum exchange over vegetated surfaces using LOTREX-10E/HIBE88 data, *Contributions to Atmospheric Physics* 63, 85–100, 1990.
- Schmidt, H. and Martin, D.: Adjoint sensitivity of episodic ozone in the Paris area to emissions on the continental scale, *J. Geophys. Res.*, 108, No. D17, ESQ 4, 1–16, 2003.
- 15 Slemr, F., Baumbach, G., Blank, P., Corsmeier, U., Fiedler, F., Friedrich, R., Habram, M., Kalthoff, N., Klemp, D., Kühlwein, J., Mannschreck, K., Möllmann-Coers, M., Nester, K., Panitz, H.-J., Rabl, P., Slemr, J., Vogt, U., and Wickert, B.: Evaluation of modelled spatially and temporally highly resolved emission inventories of photochemical precursors for the city of Augsburg: the experiment EVA and its major results, *J. Atmos. Chem.*, 42, 207–233, 2002.
- 20 Stockwell, W. R., Middleton, P., and Chang, J. S.: The second generation Regional Acid Deposition Model, chemical mechanism for regional air quality modeling, *J. Geophys. Res.*, 95, No. D10, 16 343–16 367, 1990.
- Thuburn, J. and Haine, T. W. N.: Adjoints of nonoscillatory advection schemes, *Journal of Computational Physics*, 171, 616–631, 2001.
- 25 Ustinov, E.A.: Adjoint sensitivity analysis of atmospheric dynamics: Application to the case of multiple observables, *J. Atmos. Sci.*, 58, No. 21, 3340–3348, 2001.
- Vautard, R., Beekmann, M., and Menut, L.: Applications of adjoint modelling in atmospheric chemistry: sensitivity and inverse modelling, *Environmental Modelling & Software*, 25, 703–709, 2000.
- 30 Wotawa, G., Stohl, A., and Neining, B.: The urban plume of Vienna: Comparison between aircraft measurements and photochemical model results, *Atmospheric Environment*, 32, 2479–2489, 1998.

## Appendix A: List of RADM2 transported chemical species.

Species number	Species name	Chemical formula	Symbol used in the model	Emitted species number
1	Sulfur dioxide	SO2	SO2	1
2	Sulfuric acid	H2SO4	SULF	2
3	Nitrogen dioxide	NO2	NO2	3
4	Nitric oxide	NO	NO	4
5	Ozone	O3	O3	
6	Nitric acid	HNO3	HNO3	
7	Hydrogen peroxide	H2O2	H2O2	
8	Acetaldehyde	R-CHO	ALD	5
9	Formaldehyde	CH2O	HCHO	6
10	Methyl hydrogen peroxide	CH3OOH	OP1	
11	Other organic peroxides	R-OOH	OP2	
12	Peroxyacetic acid	CH3COOOH	PAA	
13	Formic acid	HCOOH	ORA1	
14	Acetic acid	CH3COOH	ORA2	7
15	Ammonia	NH3	NH3	8
16	Dinitrogen pentoxide	N2O5	N2O5	
17	Nitrogen trioxide	NO3	NO3	
18	Peroxyacetylnitrate	CH3CO3NO2	PAN	
19	C3 to C5 alkanes	C3H8 - C5H12	HC3	9
20	C6 to C8 alkanes	C6H14 - C8H18	HC5	10
21	Other alkanes	> C10H22	HC8	11
22	Ethane	C2H6	ETH	12
23	Carbon monoxide	CO	CO	13
24	Ethene	C2H4	OL2	14
25	Terminal alkenes (propene)	e.g. C3H6	OLT	15
26	Internal alkenes (butene)	e.g. C4H8	OLI	16
27	Toluene	CH3C6H5	TOL	17
28	Xylene	(CH3)2C6H4	XYL	18
29	Acetyl peroxy radical	CH3 - CO3	ACO3	

ACPD

5, 8715–8754, 2005

### Sensitivity analysis for BERLIOZ

K. Nester and  
H.-J. Panitz

Title Page

Abstract

Introduction

Conclusions

References

Tables

Figures

◀

▶

◀

▶

Back

Close

Full Screen / Esc

Print Version

Interactive Discussion

EGU

## Sensitivity analysis for BERLIOZ

K. Nester and  
H.-J. Panitz

Title Page

Abstract

Introduction

Conclusions

References

Tables

Figures

◀

▶

◀

▶

Back

Close

Full Screen / Esc

Print Version

Interactive Discussion

EGU

### Appendix A: Continued.

Species number	Species name	Chemical formula	Symbol used in the model	Emitted species number
30	other PAN	CHOCH=CHCO <sub>3</sub> NO <sub>2</sub>	TPAN	
31	Nitrous acid	HNO <sub>2</sub>	HONO	
32	Pernitric acid	HNO <sub>4</sub>	HNO <sub>4</sub>	
33	Ketones	CH <sub>3</sub> COCH <sub>3</sub> , CH <sub>3</sub> COC <sub>2</sub> H <sub>5</sub>	KET	19
34	Glyoxal	(CHO) <sub>2</sub>	GLY	
35	Methylglyoxal	CH <sub>3</sub> COCHO	MGLY	
36	Other dicarbonyls	R-(CHO) <sub>2</sub>	DCB	
37	Other organic nitrate	R-ONO <sub>2</sub>	ONIT	
38	Cresol	HOC <sub>6</sub> H <sub>4</sub> -CH <sub>3</sub>	CSL	20
39	Isoprene	C <sub>5</sub> H <sub>8</sub>	ISO	21
40	Hydroxy radical	HO	HO	
41	Hydroperoxy radical	HO <sub>2</sub>	HO <sub>2</sub>	

## Sensitivity analysis for BERLIOZ

K. Nester and  
H.-J. Panitz

**Table 1.** Parameters modified in simplified data assimilation together with the lower and upper limits of *FacP* (reactions additionally considered in the assimilation process are denoted by an \*).

Emissions			
Classes	Species group	Species name	Limit
1	SO <sub>2</sub>	Sulfur dioxide	0.66 - 1.5
2	NO <sub>2</sub>	Nitrogen dioxide	0.66 - 1.5
3	NO	Nitric oxide	0.66 - 1.5
4	ALD+HCHO+KET	Carbonyls	0.5 - 2.0
5	HC3+HC5+HC8+ETH	Alkanes	0.5 - 2.0
6	CO	Carbon monoxide	0.5 - 2.0
7	OL2+OLT+OLI+ISO	Alkenes	0.5 - 2.0
8	TOL+XYL+CSL	Aromatics	0.5 - 2.0

Initial concentrations and boundary concentrations			
Species number in the model	Species	Limits of init. conc.	Limits of bound. conc.
3	NO <sub>2</sub>	0.75 - 1.3	0.6 - 1.4
4	NO	0.66 - 1.5	0.6 - 1.4
5	O <sub>3</sub>	0.83 - 1.2	0.6 - 1.4
9	HCHO	0.66 - 1.5	0.6 - 1.4
18	PAN	0.66 - 1.5	0.6 - 1.4
23	CO	0.66 - 1.5	0.6 - 1.4
25	OLT	0.66 - 1.5	0.6 - 1.4

Photolysis rates		
Reaction number	Photolysis reaction	Limits
1	NO <sub>2</sub> +hν→O <sub>3</sub> +NO	0.6 - 1.4
11	HCHO+hν→2HO <sub>2</sub> +CO	0.6 - 1.4
4*	HONO+hν→OH+NO	0.6 - 1.4

Reaction rates		
Rate number	Reaction	Limits
6	O <sub>3</sub> +NO→NO <sub>2</sub> +O <sub>2</sub>	0.6 - 1.4
9	HO <sub>2</sub> +NO→NO <sub>2</sub> +OH	0.6 - 1.4
24	OH+NO <sub>2</sub> →HNO <sub>3</sub>	0.6 - 1.4
29	CO+OH→HO <sub>2</sub> +CO <sub>2</sub>	0.6 - 1.4
30	CH <sub>4</sub> +OH→MO <sub>2</sub> +H <sub>2</sub> O	0.6 - 1.4
53	ACO <sub>3</sub> +NO <sub>2</sub> →PAN	0.6 - 1.4
54	PAN→ACO <sub>3</sub> +NO <sub>2</sub>	0.6 - 1.4
67	ACO <sub>3</sub> +NO→MO <sub>2</sub> +NO <sub>2</sub>	0.6 - 1.4
15*	NO+OH→HONO	0.6 - 1.4
27*	OH+HO <sub>2</sub> →H <sub>2</sub> O+O <sub>2</sub>	0.6 - 1.4
41*	HCHO+OH→HO <sub>2</sub> +CO+H <sub>2</sub> O	0.6 - 1.4
42*	ALD+OH→ACO <sub>3</sub> +H <sub>2</sub> O	0.6 - 1.4
47*	OP1+OH→0.5(MO <sub>2</sub> +HCHO+OH)	0.6 - 1.4

[Title Page](#)
[Abstract](#)
[Introduction](#)
[Conclusions](#)
[References](#)
[Tables](#)
[Figures](#)
[⏪](#)
[⏩](#)
[◀](#)
[▶](#)
[Back](#)
[Close](#)
[Full Screen / Esc](#)
[Print Version](#)
[Interactive Discussion](#)

---

**Sensitivity analysis  
for BERLIOZ**

K. Nester and  
H.-J. Panitz

---

Title Page

Abstract

Introduction

Conclusions

References

Tables

Figures

◀

▶

◀

▶

Back

Close

Full Screen / Esc

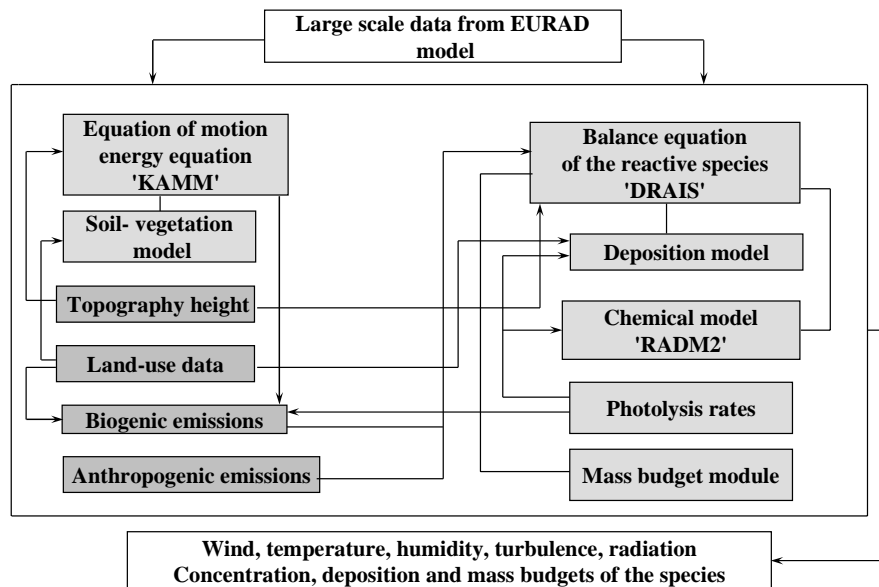
Print Version

Interactive Discussion

EGU

**Table 2.** Ranking of sensitivities.

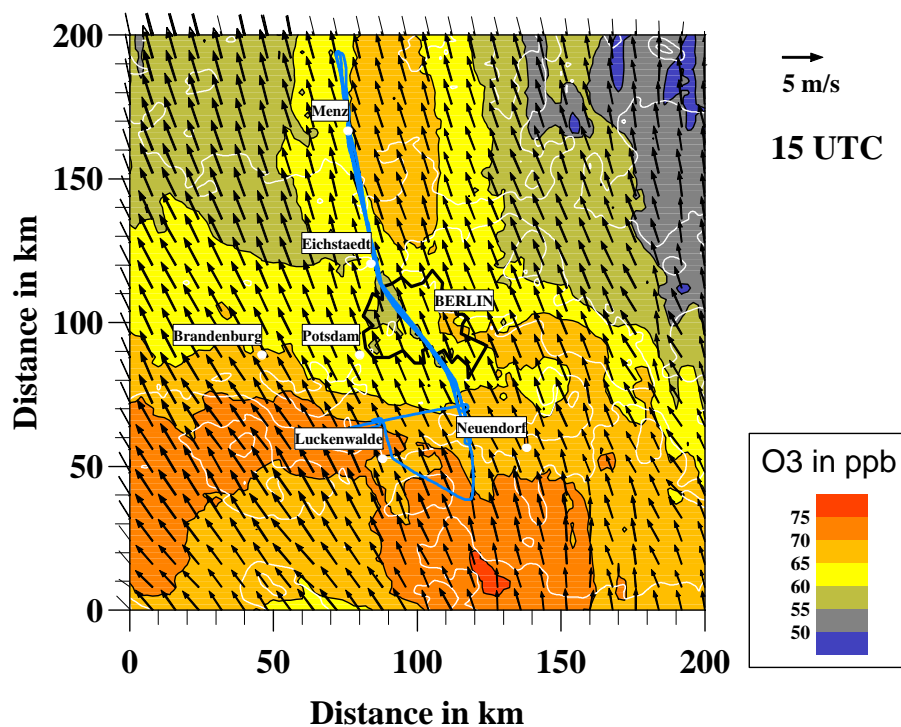
Consec. number	Sensitivity (ppb) <sup>2</sup>	Parameter
1	-171.9	Photol. rate No. 1
2	160.2	React. rate No. 6
3	159.5	NO emissions
4	-128.7	O3 bound. Cond.
5	-123.4	O3 init. cond.
6	60.1	React. Rate No. 24
7	-39.9	React. rate No. 9
8	-35.2	Photol. rate No. 11
9	-30.9	React. rate No. 54
10	-29.1	React. rate No. 67
11	-28.8	React. rate No. 30
12	28.8	React. rate No. 53
13	-26.8	OLT emissions
14	-21.6	XYL emissions
15	-18.9	React. rate No. 29
16	-18.0	OL2 emissions
17	-16.9	HC5 emissions
18	-16.4	HC3 emissions
19	-14.3	HC8 emissions
20	-10.2	CO emissions

**Sensitivity analysis  
for BERLIOZ**K. Nester and  
H.-J. Panitz

**Fig. 1.** Schematic representation of the KAMM/DRAIS model system.

[Title Page](#)[Abstract](#)[Introduction](#)[Conclusions](#)[References](#)[Tables](#)[Figures](#)[◀](#)[▶](#)[◀](#)[▶](#)[Back](#)[Close](#)[Full Screen / Esc](#)[Print Version](#)[Interactive Discussion](#)

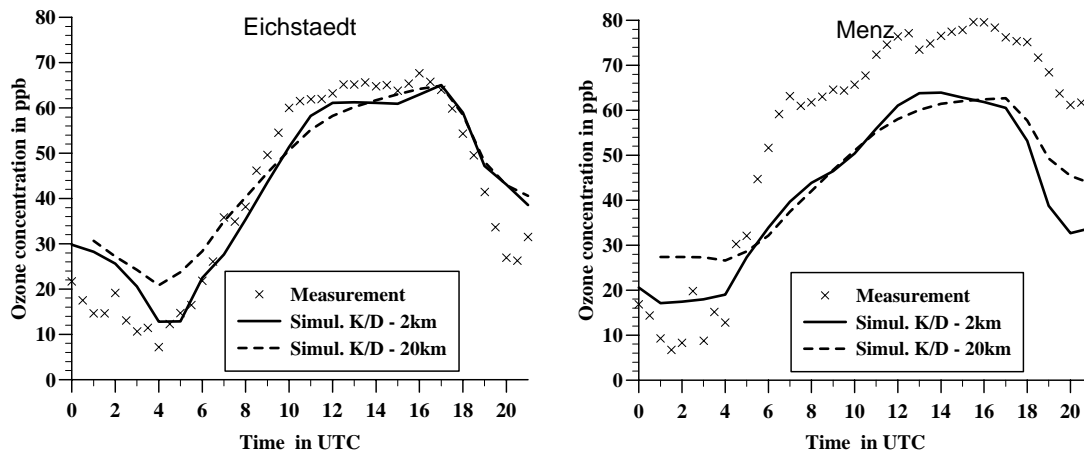
EGU

Sensitivity analysis  
for BERLIOZK. Nester and  
H.-J. Panitz

**Fig. 2.** Wind distribution and ozone concentration distribution near ground level for 20 July 1998 and afternoon flight track (thick blue line) of the IBUG aircraft.

[Title Page](#)[Abstract](#)[Introduction](#)[Conclusions](#)[References](#)[Tables](#)[Figures](#)[◀](#)[▶](#)[◀](#)[▶](#)[Back](#)[Close](#)[Full Screen / Esc](#)[Print Version](#)[Interactive Discussion](#)

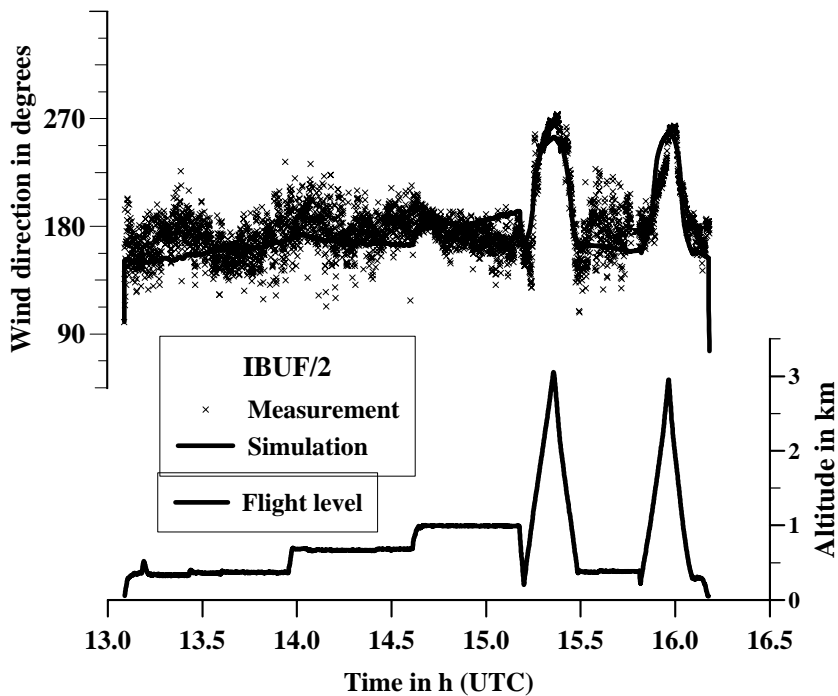
EGU

**Sensitivity analysis  
for BERLIOZ**K. Nester and  
H.-J. Panitz

**Fig. 3.** Diurnal cycle of ozone concentration measured at ground level for the Eichstaedt and Menz stations compared to the results simulated with 2 km and 20 km grid resolution (see Sect. 3.2).

[Title Page](#)[Abstract](#)[Introduction](#)[Conclusions](#)[References](#)[Tables](#)[Figures](#)[◀](#)[▶](#)[◀](#)[▶](#)[Back](#)[Close](#)[Full Screen / Esc](#)[Print Version](#)[Interactive Discussion](#)

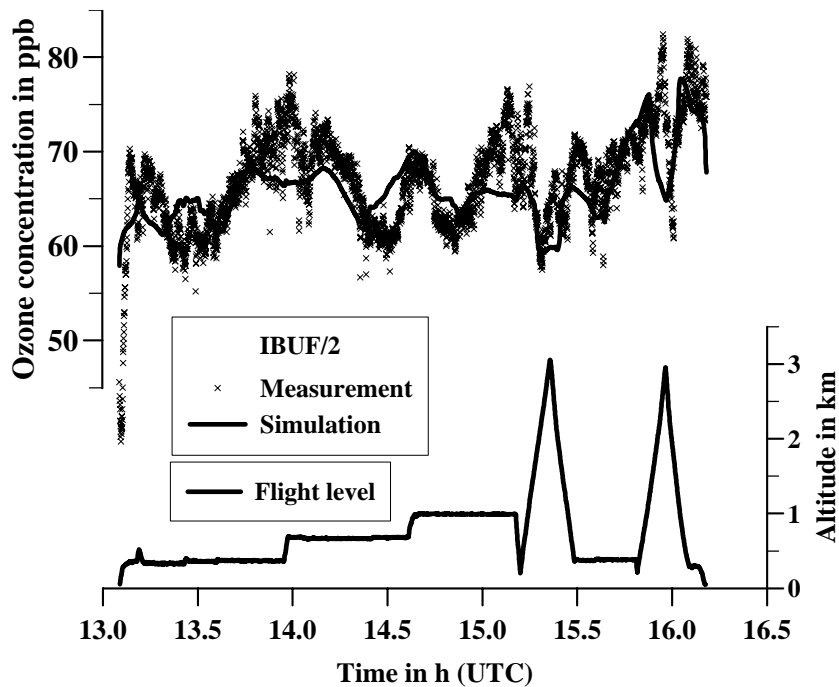
EGU

Sensitivity analysis  
for BERLIOZK. Nester and  
H.-J. Panitz

**Fig. 4.** Comparison of wind direction along the flight track of IBUG.

[Title Page](#)[Abstract](#)[Introduction](#)[Conclusions](#)[References](#)[Tables](#)[Figures](#)[◀](#)[▶](#)[◀](#)[▶](#)[Back](#)[Close](#)[Full Screen / Esc](#)[Print Version](#)[Interactive Discussion](#)

EGU

**Sensitivity analysis  
for BERLIOZ**K. Nester and  
H.-J. Panitz**Fig. 5.** Comparison of ozone concentration along the flight track of IBUF.[Title Page](#)[Abstract](#)[Introduction](#)[Conclusions](#)[References](#)[Tables](#)[Figures](#)[◀](#)[▶](#)[◀](#)[▶](#)[Back](#)[Close](#)[Full Screen / Esc](#)[Print Version](#)[Interactive Discussion](#)

EGU

## Sensitivity analysis for BERLIOZ

K. Nester and  
H.-J. Panitz

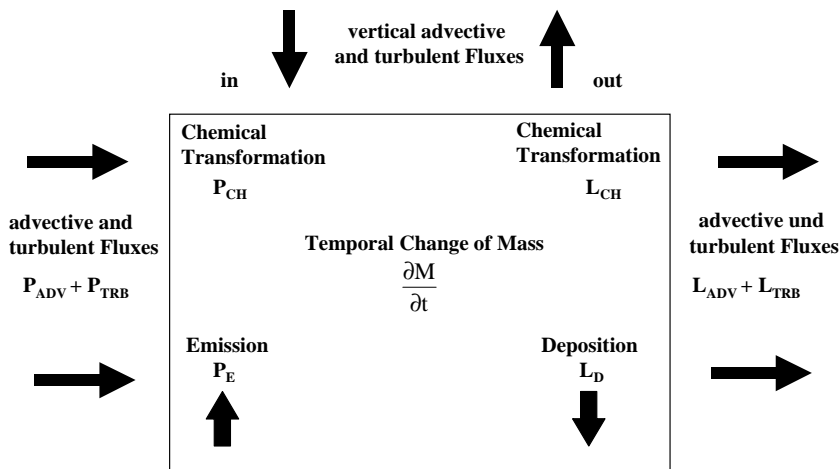


**Fig. 6.** Illustration of mass budget components.

Title Page

Abstract

Introduction

Conclusions

References

Tables

Figures

◀

▶

◀

▶

Back

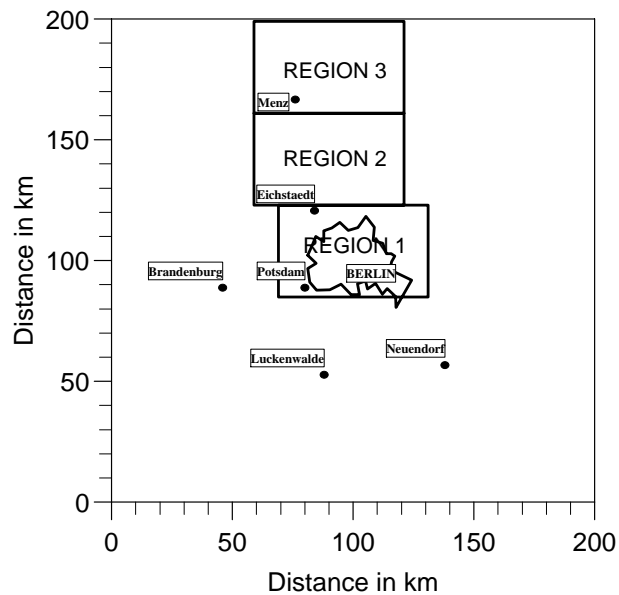
Close

Full Screen / Esc

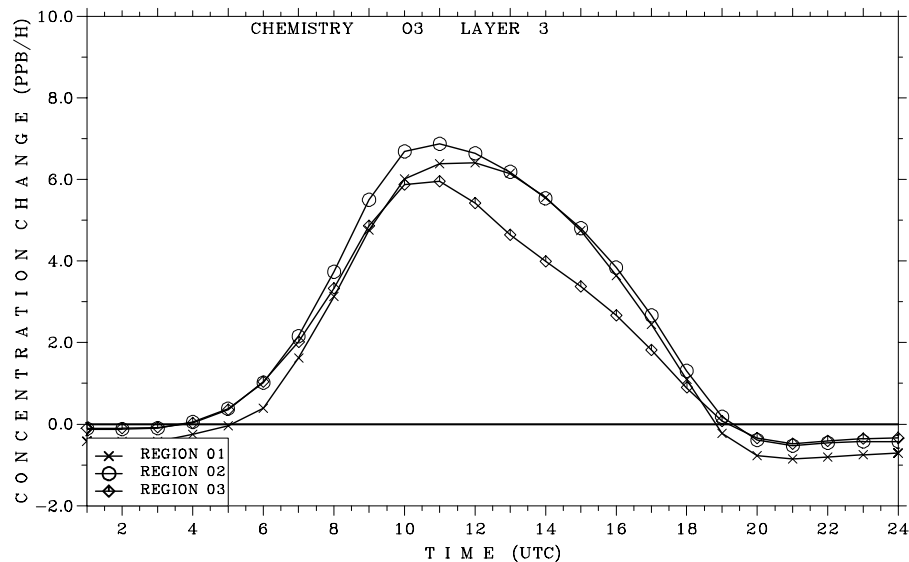
Print Version

Interactive Discussion

EGU

**Sensitivity analysis  
for BERLIOZ**K. Nester and  
H.-J. Panitz**Fig. 7.** Arrangement of regions.[Title Page](#)[Abstract](#)[Introduction](#)[Conclusions](#)[References](#)[Tables](#)[Figures](#)[◀](#)[▶](#)[◀](#)[▶](#)[Back](#)[Close](#)[Full Screen / Esc](#)[Print Version](#)[Interactive Discussion](#)

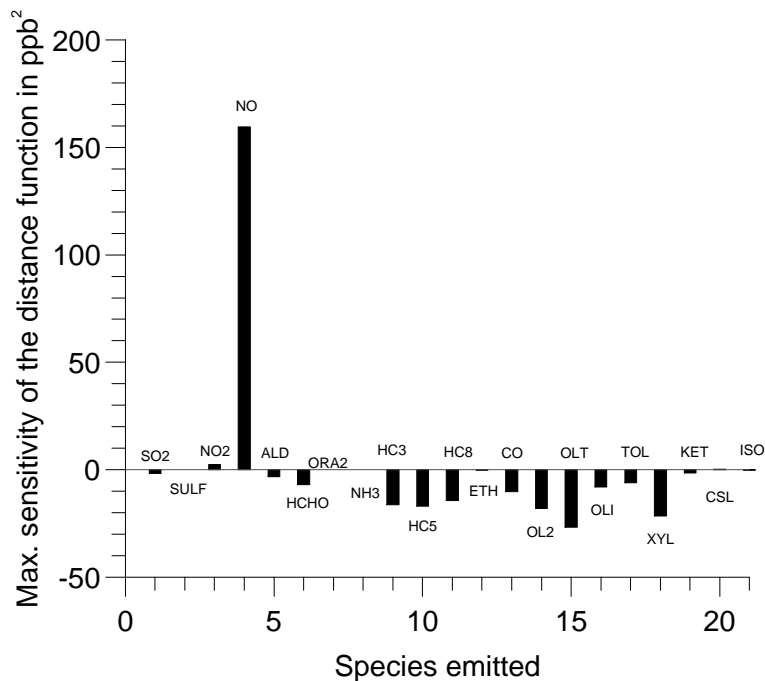
EGU

**Sensitivity analysis  
for BERLIOZ**K. Nester and  
H.-J. Panitz

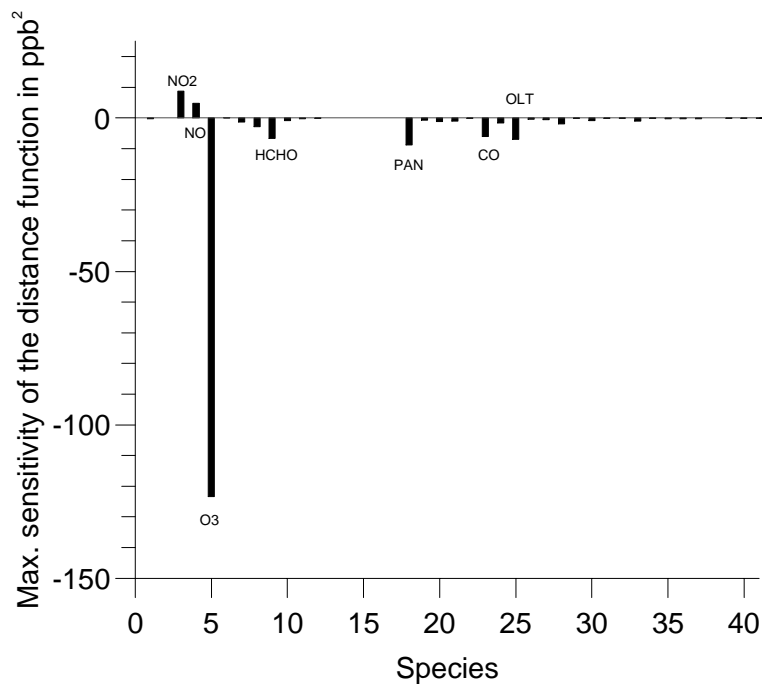
**Fig. 8.** Diurnal cycle of ozone production rate caused by chemical reactions in layer 3 over three regions.

[Title Page](#)[Abstract](#)[Introduction](#)[Conclusions](#)[References](#)[Tables](#)[Figures](#)[◀](#)[▶](#)[◀](#)[▶](#)[Back](#)[Close](#)[Full Screen / Esc](#)[Print Version](#)[Interactive Discussion](#)

EGU

**Sensitivity analysis  
for BERLIOZ**K. Nester and  
H.-J. Panitz**Fig. 9.** Maximum sensitivity of the distance function ( $S_{ef}$ ) related to the emissions ( $F_{acE}$ ).[Title Page](#)[Abstract](#)[Introduction](#)[Conclusions](#)[References](#)[Tables](#)[Figures](#)[◀](#)[▶](#)[◀](#)[▶](#)[Back](#)[Close](#)[Full Screen / Esc](#)[Print Version](#)[Interactive Discussion](#)

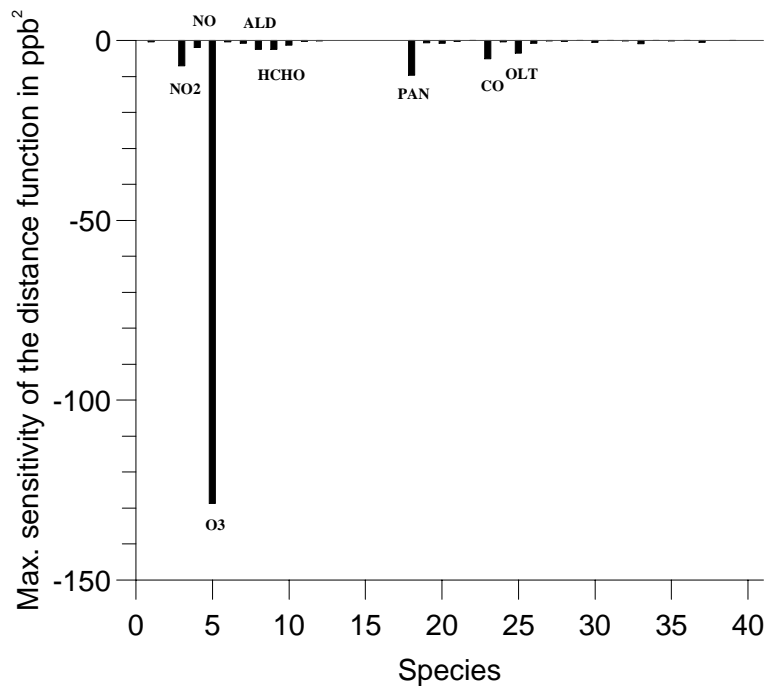
EGU

**Sensitivity analysis  
for BERLIOZ**K. Nester and  
H.-J. Panitz

**Fig. 10.** Maximum sensitivity of the distance function ( $S_{if}$ ) related to the initial conditions ( $F_{acI}$ ).

[Title Page](#)[Abstract](#)[Introduction](#)[Conclusions](#)[References](#)[Tables](#)[Figures](#)[◀](#)[▶](#)[◀](#)[▶](#)[Back](#)[Close](#)[Full Screen / Esc](#)[Print Version](#)[Interactive Discussion](#)

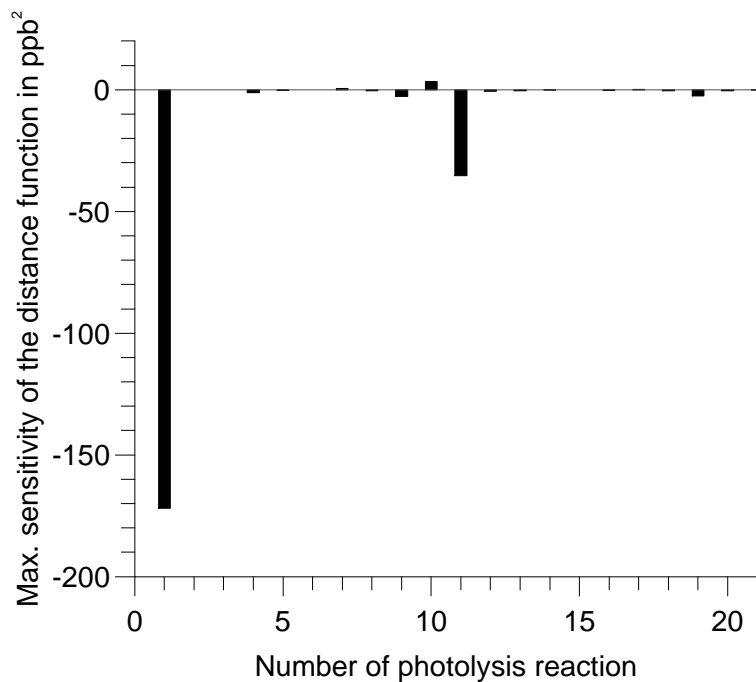
EGU

**Sensitivity analysis  
for BERLIOZ**K. Nester and  
H.-J. Panitz

**Fig. 11.** Maximum sensitivity of the distance function ( $S_{bf}$ ) related to the boundary conditions ( $FacB$ ).

[Title Page](#)[Abstract](#)[Introduction](#)[Conclusions](#)[References](#)[Tables](#)[Figures](#)[◀](#)[▶](#)[◀](#)[▶](#)[Back](#)[Close](#)[Full Screen / Esc](#)[Print Version](#)[Interactive Discussion](#)

EGU

**Sensitivity analysis  
for BERLIOZ**K. Nester and  
H.-J. Panitz

**Fig. 12.** Maximum sensitivity of the distance function ( $Spf$ ) related to the photolysis rates ( $FacP$ ).

[Title Page](#)[Abstract](#)[Introduction](#)[Conclusions](#)[References](#)[Tables](#)[Figures](#)[◀](#)[▶](#)[◀](#)[▶](#)[Back](#)[Close](#)[Full Screen / Esc](#)[Print Version](#)[Interactive Discussion](#)

EGU

**Sensitivity analysis  
for BERLIOZ**K. Nester and  
H.-J. Panitz

Title Page

Abstract

Introduction

Conclusions

References

Tables

Figures

◀

▶

◀

▶

Back

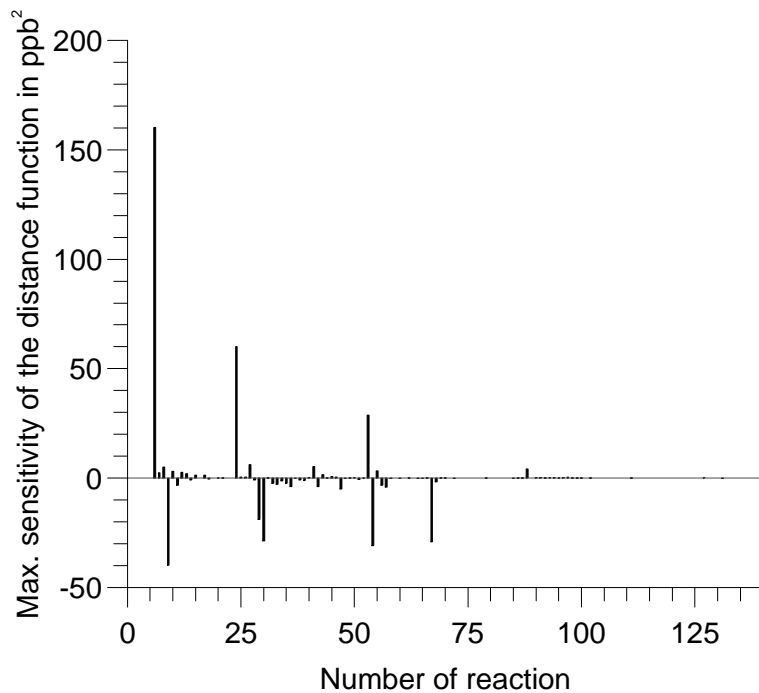
Close

Full Screen / Esc

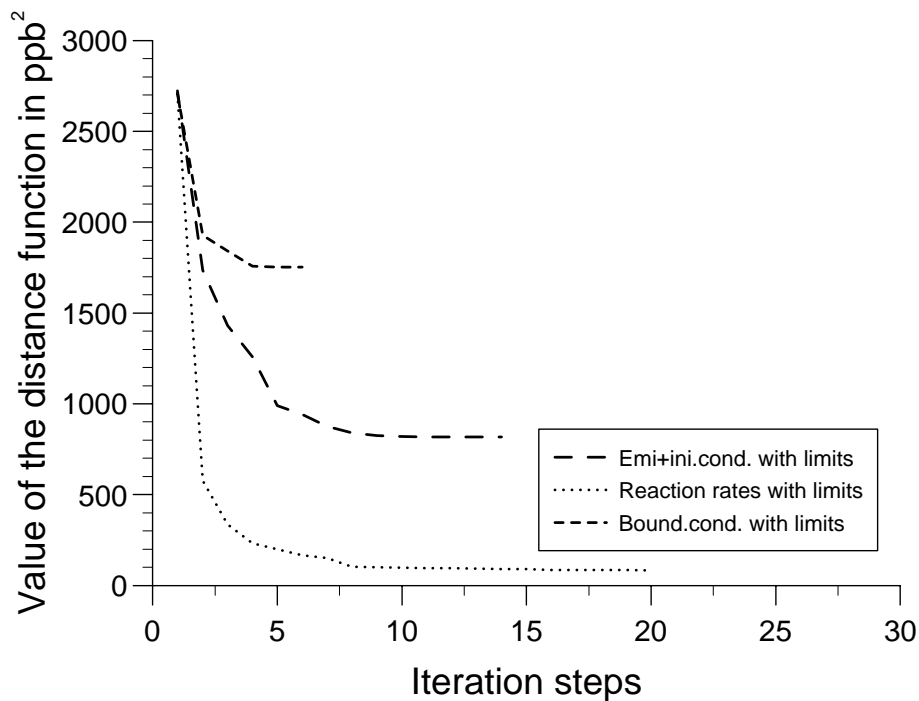
Print Version

Interactive Discussion

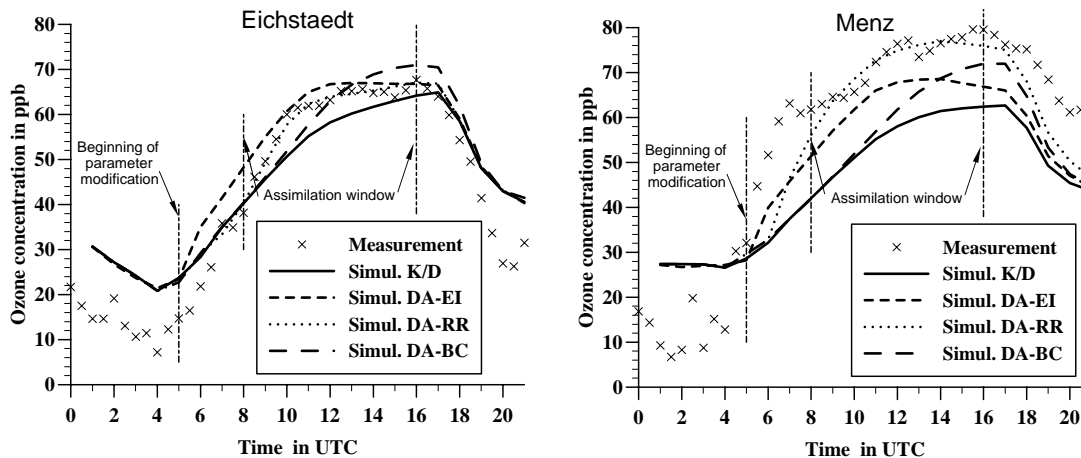
EGU



**Fig. 13.** Maximum sensitivity of the distance function ( $S_{rf}$ ) related to the reaction rates ( $F_{acR}$ ).

**Sensitivity analysis  
for BERLIOZ**K. Nester and  
H.-J. Panitz**Fig. 14.** Iterative reduction of the distance function.[Title Page](#)[Abstract](#)[Introduction](#)[Conclusions](#)[References](#)[Tables](#)[Figures](#)[◀](#)[▶](#)[◀](#)[▶](#)[Back](#)[Close](#)[Full Screen / Esc](#)[Print Version](#)[Interactive Discussion](#)

EGU

Sensitivity analysis  
for BERLIOZK. Nester and  
H.-J. Panitz

**Fig. 15.** Diurnal cycle of the ozone concentration at ground level for the stations of Eichstaedt and Menz (K/D : Reference case with 20 km resolution, DA : Data assimilation, EI : Emissions and Initial concentrations; RR : Photolysis – and other Reaction Rates; BC : Boundary concentrations).

Title Page

Abstract

Introduction

Conclusions

References

Tables

Figures

◀

▶

◀

▶

Back

Close

Full Screen / Esc

Print Version

Interactive Discussion

EGU